ORIGINAL ARTICLE

Evolution of the French Guiana coast from Late Pleistocene to Holocene based on chenier and beach sand dating

Guillaume Brunier[1] · Toru Tamura[2,3] · Edward J. Anthony[4,1] · Philippe Dussouillez[4] · Antoine Gardel[1]

Abstract
The 1500-km-long Guianas coast between the Amazon delta in Brazil and the Orinoco delta in Venezuela is characterized by alternations of muddy shoreline advance and retreat caused by large mud banks migrating alongshore from the mouths of the Amazon. In this dominantly muddy environment, wave reworking of sand and shells results in the formation of beaches, termed 'cheniers', that provide valuable information on coastal evolution, especially on past erosional phases. Twenty-eight depositional ages showing the long-term patterns of shoreline mobility in French Guiana were obtained from optically stimulated luminescence. Twenty-one ages younger than 7 ka define three clusters centred on 4.5 ka, 1.0–1.3 ka, and 0.30 ka. They indicate that chenier formation was relatively synchronous and significantly affected by alongshore diversions of river mouths and changes in river-mouth position over time under the influence of muddy shoreline advance. A prominent cluster at 1.0–1.3 ka reveals a clear hiatus after the 4.5 ka cluster, indicating that the present muddy coastal plain of French Guiana was largely formed and preserved after 1.0–1.3 ka. This cluster also implies either an episode of coastal retreat or no coastal advance around 1.0–1.3 ka. The remaining seven samples were derived from Late Pleistocene deposits of headland-bound beaches and probable cheniers capped by aeolian sand, suggesting similar conditions of coastal Amazon mud-dominated sedimentation. By informing on past patterns of shoreline mobility, these results have broader implications for coastal land-use planning and shoreline management between the mouths of the Amazon and Orinoco Rivers.

Keywords Amazon-influenced coast · Chenier · Coastal erosion · Mud bank · Optically stimulated luminescence dating · French Guiana

✉ Guillaume Brunier
   guillaume_brunier@hotmail.fr

1   UAR LEEISA, CNRS, Ifremer, Université de Guyane, Cayenne, French Guiana

2   Geological Survey of Japan, AIST, Tsukuba, Ibaraki 305-8567, Japan

3   Graduate School of Frontier Sciences, The University of Tokyo, Kashiwa, Chiba 277-8561, Japan

4   UM 34 CEREGE, Aix Marseille Université, CNRS, IRD, INRAE, Collège de France, Aix-en-Provence, France

Introduction

Cheniers are beach deposits composed of sand, shells, and gravel that are reworked by waves over a muddy substrate (Otvos and Price 1979; Otvos 2018). Cheniers are much less common than classical beach ridges (Scheffers et al. 2012; Tamura 2012), because their formation requires, in addition to adequate wave energy to rework the coarse-grained sediments into coherent beach deposits, the presence of abundant cohesive sediments (e.g. Nardin and Fagherazzi 2018; Anthony et al. 2019). Conditions for chenier formation are generally best met in river deltas (e.g. Saito et al. 2000; Hori et al. 2001; van Maren 2005; McBride et al. 2007) and adjacent to some estuaries (e.g. Anthony 1989; Hein et al. 2016), but cheniers can also be formed in other coastal environments wherever coarse sediment is reworked by waves into coherent deposits and segregated from mud (e.g. Woodroffe and Grime 1999; Tas et al. 2020, 2022).

Cheniers may occur as individual ridges but are more commonly organized in bands or bundles of multiple ridges, referred to as chenier plains (Otvos 2018). Cheniers, like other coastal, wave-formed deposits, can provide a variety of ecosystem services, such as energy dissipation and protection of backshore areas. By virtue of their elevation and alongshore continuity, cheniers also commonly host settlements and routes. They generally provide material for radiometric dating of coastal deposits

and can, thus, serve, like beach ridges (Tamura 2012), as environmental archives.

The coast of French Guiana (Fig. 1) is part of the mud-dominated 1500-km-long Atlantic Guianas coast of northern South America between the mouths of the Amazon in Brazil and those of the Orinoco in Venezuela. This muddy coast comprises cheniers occurring individually or in bundles (Fig. 1). Presently active cheniers serve as major beach nesting sites for critically endangered marine turtles and
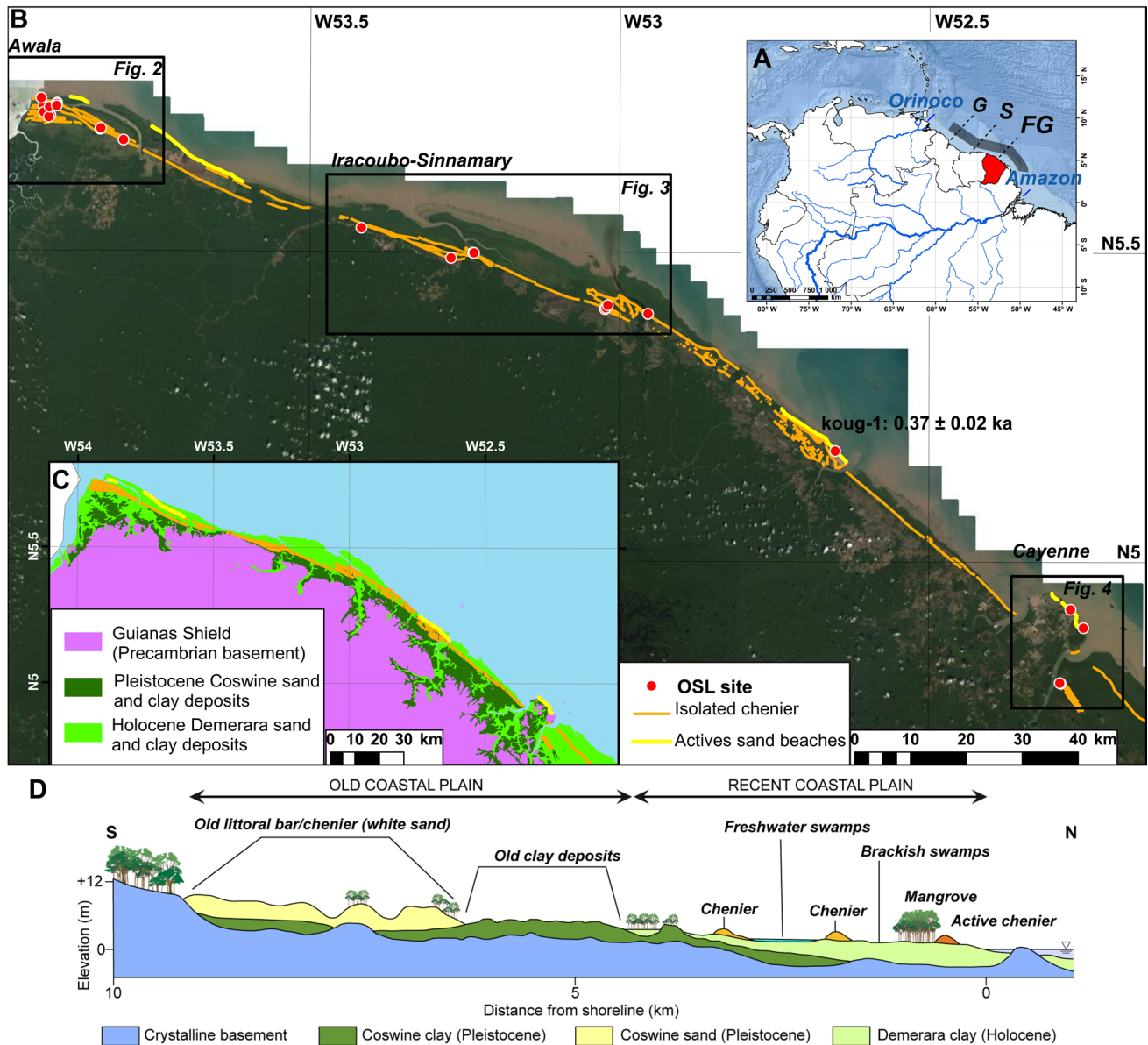

Fig. 1 (A) The Amazon-influenced Guianas coast between the mouths of the Amazon and the Orinoco Rivers, with French Guiana (FG) highlighted in red (S = Suriname, G = Guyana). Thick grey line depicts the Amazon mud bank belt. (B) 2015 SPOT 6 satellite image of the study area showing locations of optically stimulated luminescence (OSL) samples (red dots) and cheniers (orange lines) extracted from geological maps (1994) and soil maps (1975). Present beaches are shown by yellow lines. An OSL age determined for sample gsj15181 taken at Kou-1, a chenier facing the present beach, is shown. (C) Simplified geological map highlighting Holocene and Pleistocene deposits of the present coastal plain, adapted from a geological map (2001). (D) Cross-section of typical stratigraphic units in western French Guiana (from Prost, 1989)

provide various ecosystem services, including the protection of wetlands, and sites for the location of numerous villages, towns, and coastal roads. They are also exploited as quarries for aggregate used in the construction of houses and roads. Although these cheniers have been described in numerous previous studies and considered spanning both the Pleistocene and Holocene (Brinkman and Pons 1968; Augustinus 1978; Augustinus et al. 1989; Daniel 1989; Prost 1989; Wong et al. 2009; Anthony et al. 2010, 2019; Brunier et al., 2019), nothing is known of the time frame of their formation and their phases of development as expressed by their spatio-temporal distribution over the Guianas coastal plain. In order to gain insight on these aspects of chenier formation and development, a total of twenty-eight optically stimulated luminescence (OSL) ages were determined on cheniers and sandy deposits studding the French Guiana coastal plain.

Study area and context of chenier formation

The Guianas coast is exposed to trade-wind waves throughout the year (Gratiot et al. 2007). It is the terminus of numerous rivers (Gardel et al., this issue) draining the Andes, the Andean foreland, the Llanos, and the Guiana Shield (Fig. 1). By far the most important of these rivers is the Amazon. Sediment supply from the Amazon has dominated the geological development of this coast (Brinkman and Pons 1968; Augustinus 1978; Prost, 1989; Wong, 1992; Wong et al. 2009; Anthony et al. 2010, 2014; Nittrouer et al. 2021). Mud supplied by the Amazon is organized into individual coastal banks that migrate towards the northwest under the influence of waves and currents, thus forming an alongshore sediment dispersal and depositional system unique in the world. Each mud bank can be up to 5 m thick, 10 to 60 km long, and 20 to 30 km wide (Gardel and Gratiot 2005) and can contain several times the annual mud supply of the Amazon (Anthony et al. 2014). A bank migrating alongshore efficiently dissipates wave energy (Wells and Coleman 1981; Gratiot et al. 2007; Winterwerp et al. 2007; de Vries et al., 2022) and is separated from neighbouring banks by inter-bank areas where, in the absence of wave dissipation induced by mud banks, energetic incident waves can reach the coast and cause erosion.

Since the mud banks migrate alongshore, the shoreline at any point will vary over time between bank (mud accumulation) and inter-bank (erosion) phases. Active cheniers are formed only in inter-bank areas where the incident wave energy is relatively high. They can become isolated from the sea and preserved inland through growth of the muddy coastal plain. The formation of cheniers is, therefore, not primarily related to temporal (commonly seasonal) alternations of low wave energy conditions (muddy sedimentation)

and stormy or high wave energy conditions (chenier formation), the case for most of the world's chenier coasts, but depends foremost on the alongshore alternations of banks and inter-bank zones. Each inter-bank erosion phase can result in the partial, or rarely, total loss, especially during high wave-energy seasons associated with NAO and El Niño years (Gratiot et al. 2007; Walcker et al. 2015), of the shoreline advance gained by coastal plain during a previous bank phase (Allison and Lee 2004). More commonly, erosion of the coastal plain is partial, signifying that there has been a net growth over the last 6000–7000 years that has also led to the isolation of wave-formed cheniers (Fig. 1; Augustinus 1978, 2004; Augustinus et al. 1989; Prost 1989; Allison and Lee 2004; Wong et al. 2009). The geological history of this coastal plain also includes Pleistocene deposits that commonly occur inland of the Holocene plain (Brinkman and Pons 1968; Wong et al. 2009), thus possibly suggesting similar conditions of Pleistocene muddy sedimentation and chenier formation.

Milne et al. (2005) reconstructed the sea-level curve in Suriname by compiling radiocarbon dates of coastal mangrove swamps reported by Roeleveld and Van Loon (1979). While the data possibly contain errors introduced by uncertainties in elevations of the sample sites and by the effect of sediment compaction, they show that sea level rose from − 6 m at 8.5 cal ka BP to around 0 m by 6 cal ka BP, followed by no significant fluctuations until present.

Methods

Fieldwork and chenier sediment sampling

Two field surveys were carried out, respectively on 17–20 October 2014 and 10–16 October 2015. Five study areas were selected for sampling: Awala, Irracoubo, Sinnamary, Kourou, and Remire in the capital city of Cayenne, from west to east, covering the entire French Guiana coast (Fig. 1). Sediment samples for OSL dating were collected from auger boreholes and outcrops. Auger boreholes up to 2.2 m deep were dug at 20 sites (Table S1). Light-unexposed samples were obtained by hammering stainless-steel tubes into the bottom of the holes. Once the tube was recovered, both ends were capped with plastic lids to prevent further exposure to light. Sediment grain size and colour were observed and logged during the auger drilling. Sediment samples were also collected by hammering plastic tubes into outcrop surfaces at four sites. Sedimentological observation was made at these outcrop sections. A real-time kinematic (RTK) GPS topographic survey was carried out on the Remire section to obtain the elevation profile of the sampled outcrop. The Universal Transverse Mercator (UTM) 22 North zone based on Réseau Géodésique Francais Guyane 1995 (RGFG)

datum was used as the geographical coordinate system and the Earth Gravitational Model (EGM) 2008 as the vertical datum of elevation measures.

The surficial geology of the chenier locations was identified from maps at the 1/50,000 scale produced by the French Geological Survey (BRGM) in 1994, complemented by soil maps of French Research Institute for Development (IRD) at the 1/10,0000 scale edited in 1975. These maps were georeferenced in the Centre Spatial Guyanais (CSG) 1967 datum, retained as the native datum, and were then converted to UTM 22 N RGFG 1995. The geological map at the 1/50,000 scale displayed in Fig. 1 was compiled from the BRGM Infoterre database (infoterre.brgm.fr) and vectorized from original maps with the UTM 22 N RGFG 1995 datum.

Optically stimulated luminescence dating

The preparation of the samples and the OSL dating measurements were carried out at the luminescence laboratory of the Geological Survey of Japan. In order to avoid contamination of the quartz OSL signals, the samples were prepared under controlled red light. Sediment within 20–25 mm of the ends of the tube was removed and used for measurements of water content and dosimetry. Quartz grains of 90–120, 120–180, or 180–250 μm in diameter were extracted from bulk samples following the method of Bateman and Catt (1996). Monolayers of quartz were mounted on 9.8-mm-diameter disks to form large aliquots, which were then measured with a TL-DA-20 automated Risø TL/OSL reader equipped with blue LEDs for stimulation and a ^{90}Sr/^{90}Y beta source for laboratory irradiation. Emitted OSL through a Hoya U-340 filter was measured with a photomultiplier.

To monitor and correct for sensitivity changes, the single-aliquot regenerative-dose (SAR) protocol was used to determine the equivalent dose (D_e) using the OSL response to a test dose (Murray and Wintle 2000). OSL measurements were made at 125 °C. The OSL intensity was determined by integrating the signal for an initial 0.5 s subtracted from the background signal observed over 15–20 s after the onset of stimulation. In all samples, a bright natural OSL signal was observed, and a dose response curve was defined to estimate D_e. Feldspar contamination was checked by using the IR test during preliminary measurements. The IR test results suggested the presence of a slight feldspar signal in relatively young samples even after re-etching with hydrofluoric acid. Therefore, we added an IR stimulation step at 50 °C for 40 s prior to each OSL stimulation to remove the feldspar signal (Banerjee et al. 2001), except for the seven oldest samples. Preheat dose recovery and plateau tests were carried out on samples gsj15193, gsj14110, and gsj14105, which represent the Holocene coastal sand in the western sector of French Guiana, Holocene sand in the eastern sector, and Pleistocene sand, respectively, by changing the preheat temperature from

160 to 260 °C in 20 °C increments (Fig. S1). Lower preheat temperature resulted in poor recovery and recycling ratios outside 1.0 ± 0.1 in some samples, while temperatures higher than 240 °C were acceptable. Thus, a preheat temperature of 240 °C was chosen. A 160 °C cut-heat for the OSL response to the test dose was used for all samples. To determine D_e, six regeneration points were measured, including 0 Gy and a replicate of the first regeneration point, which was used to check whether the sensitivity correction procedure was performing adequately. Data from aliquots were rejected when recycling ratios were outside 1.0 ± 0.1. Statistical outliers were also removed based on the criterion that aliquots with D_e outside the 25th and 75th percentiles of the mean are discarded (Boulter et al. 2010). We measured 16–34 aliquots per sample. The final D_e value was determined by applying the Central Age Model (Galbraith et al. 1999).

Determination of the environmental dose rate was carried out based on the contributions of both natural radio-isotopes and cosmic radiation (Table S1). Concentrations of potassium, uranium, thorium, and rubidium were quantified through inductively coupled plasma mass spectrometry and were converted to dose rate based on data from Adamiec and Aitken (1998). Past changes of water content are not known, so an uncertainty margin of 5% was applied to the measured water content values ranging from 1 to 30%. The cosmic dose rate was estimated based on Prescott and Hutton (1994). All reported OSL ages are expressed relative to AD 2015.

Results and interpretation

Geomorphology and stratigraphy

Awala area

The coastal lowland in the Awala area is 8–10 km wide and characterized by complex traces of cheniers and former courses of the Mana River (catchment area: 12,090 km^2) deflected westwards towards the mouth of the larger (catchment area: 66,184 km^2) Maroni River (Fig. 2A). A cluster of six to seven chenier ridges stretching E-W impinges on the east bank of the Maroni River mouth. The northeastern boundary of this cluster is defined by an abandoned channel of the Mana River with the subtle development of a natural levee. Seaward of the abandoned channel occur two to five chenier ridges parallel to the present shore. These shore-parallel ridges taper off towards the Maroni River mouth and are partly truncated by a meander of the Mana River.

Sediment samples for OSL dating were collected from an outcrop section and 11 auger holes in this area (Fig. 2B). The outcrop at Sim-1, exposed in a beach scarp in the north-western end of the tapering chenier, shows a well-defined
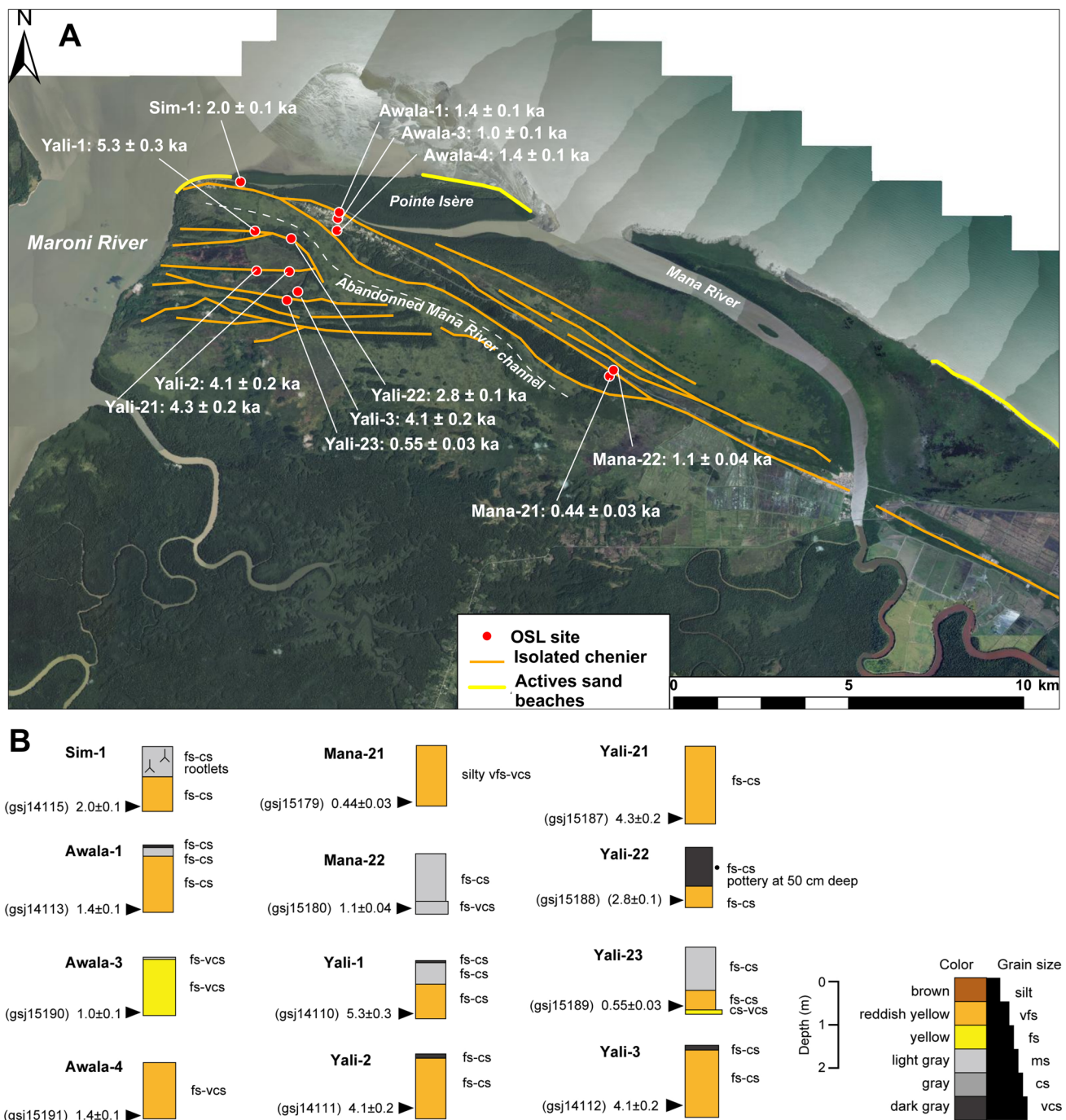
Fig. 2 (**A**) Orthophotograph from 2018 of the Awala area. Chenier ridges and optically stimulated luminescence (OSL) sample sites are highlighted. (**B**) Sediment logs recorded during the auger drilling and characterized by outcrop observation at Sim-1. The sediment log legend is vfs, very fine sand; fs, fine sand; ms, medium sand; cs, coarse sand; vcs, very coarse sand

podzol succession of chenier sediments characterized by reddish yellow, poorly sorted, fine to coarse sands (Fig. 2B). Sample gsj14115 was taken from this reddish yellow unit. Along the shore-parallel ridge and about 2 km southeast of Sim-1, samples gsj15191, 15,192, and 14,113 were collected from auger holes at Awala-4, -3, and -1, respectively.

Auger holes at Mana-21 and -22 were located 10 km further southeast, where samples gsj15179 and 15,180 were collected, respectively. Auger holes were also drilled to collect samples gsj15188, 14,112, 14,111, 15,187, and 14,110, at Yali-22, -3, -2, -21, and -1, respectively, along the right bank of the Maroni River. Sample gsj15189 was also collected

from the auger hole at Yali-23 located on the subtle levee along the abandoned channel. The stratigraphy observed in these auger holes is generally characterized by reddish yellow fine to coarse sand which, at several sites, underlies light grey leached fine to coarse sand and a thin dark grey organic topsoil. An exception is identified at Yali-22, where the topsoil is up to 80 cm thick and contains fragments of pottery.

Irracoubo and Sinnamary areas

The Irracoubo and Sinnamary areas span a 70-km-long sector of the central French Guiana coast, punctuated by two rivers, the Irracoubo (catchment area: 2500 km^2) and Sinnamary (catchment area: 6565 km^2), the courses of which are deflected westwards for several kilometres (Fig. 3A). The coastal lowland is < 7 km wide and tends to be broader and narrower in the eastern and western sides of the river mouths, respectively, reflecting the sporadic nature of muddy shoreline advance associated with past occurrence

of mud banks migrating alongshore. Much of the lowland is marsh with limited occurrences of chenier ridges at the inland boundary except for the left bank of the river channels, where three to four shore-parallel ridges are present.

Sediment sampling was carried out at an outcrop section and six auger holes in the Iracoubo and Sinnamary areas (Fig. 3B). The outcrop at Ira-4 was exposed in a trench dug for road construction and showed a section of homogenous very fine yellow sand to granules. Samples gsj15173 and 15,174 were collected from different levels at Ira-4. Auger holes at Ira-1 and -3 were located on the chenier ridge bounding the landward margin of the coastal lowland, where samples gsj15170 and 15,172 were collected from reddish yellow fine sand, respectively. Auger holes were drilled at Sinnamary-1, -2, and -3 in a series of chenier ridges on the west bank of the Sinnamary River. The stratigraphy at these sites is different from that of other sites. At Sinnamary-1 and -3, silty very fine sand to sandy silt was observed at the base of auger holes and overlain
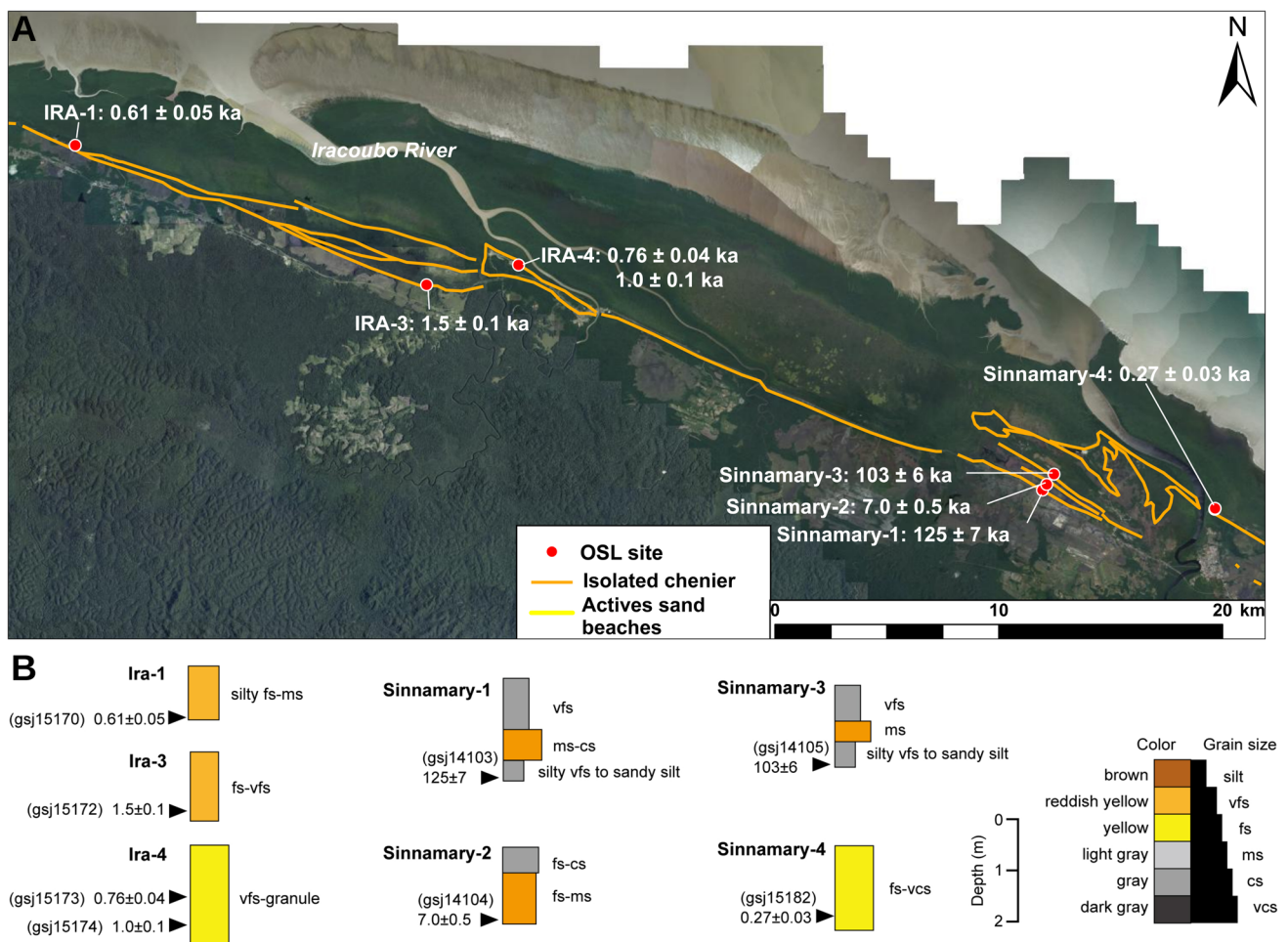

Fig. 3 (**A**) Orthophotograph from 2018 of the Iracoubo–Sinnamary area. Locations of optically stimulated luminescence (OSL) sample sites are shown by red dots. (**B**) Sediment logs recorded during the auger drilling

by reddish yellow medium to coarse sand and leached light grey fine sand. Samples gsj14103 and 14,105 were taken from the silty layer at Sinnamary-1 and -3, respectively. The auger hole at Sinnmary-2 did not reach the silty layer and revealed a stratigraphy of reddish yellow fine to medium sand overlain by leached light grey fine to coarse sand. Sample gsj14104 was collected from the reddish sand. On the chenier ridge of the east bank of the Sinnamary River, sample gsj15182 was obtained from yellow fine to very coarse sand drilled at Sinnamary-4.

Cayenne and Kourou areas

The Cayenne and Kourou areas form the only two bedrock promontories cropping out on the present shore along the muddy 1500-km-long Amazon-Orinoco coast (Figs. 1, 4A). Other small outcrops occur as islets and rock masses not far out at sea. Cayenne city lies on the west bank of the Mahury River, and Kourou city (site of the European Space Agency satellite launching pad in South America) is on the west bank of the Kourou River (catchment area: 2000 km^2). These promontories are part of the Precambrian Guiana Shield, and are formed of igneous rocks, notably diorite and granite, but also incorporate Pleistocene marine deposits (Janjou,

2004). The two promontories are largely fronted by rocky shores with pocket beaches. Coastal outcrops at Montjoly and Remire beaches were investigated in Cayenne. At the outcrop section, on a backshore bluff on Montjoly beach, reddish yellow massive silt 1.4-m-thick was observed, and an OSL sample was collected from the basal part of the outcrop. The outcrop section at Remire beach ranges from + 3.0 to + 7.4 m in elevation (Figs. 2C, 4B). The basal part of the section, 0.7 m thick, is light grey or reddish-yellow fine to coarse sand with parallel lamination characterized by pronounced heavy mineral concentrations. The laminated sand is overlain by reddish-yellow massive sandy silt of which the upper part contains scattered pebbles. Samples gsj14106 and 14,107 were collected from the laminated sand and samples gsj14108 and 14,109 from the massive sandy silt.

The muddy coastal plain along the east bank of the Mahury River is up to 25 km wide and largely occupied by marshes (Fig. 4A). This eastern extremity of the French Guiana coast is contiguous with the Amapa coast of Brazil, characterized by large mud capes diverting river mouths (Gardel et al., this issue). A few distinct shore-parallel chenier ridges occur 10–12 km inland from the present shoreline east of the Mahury. A subtle ridge is also present closer to the shoreline. Auger holes were
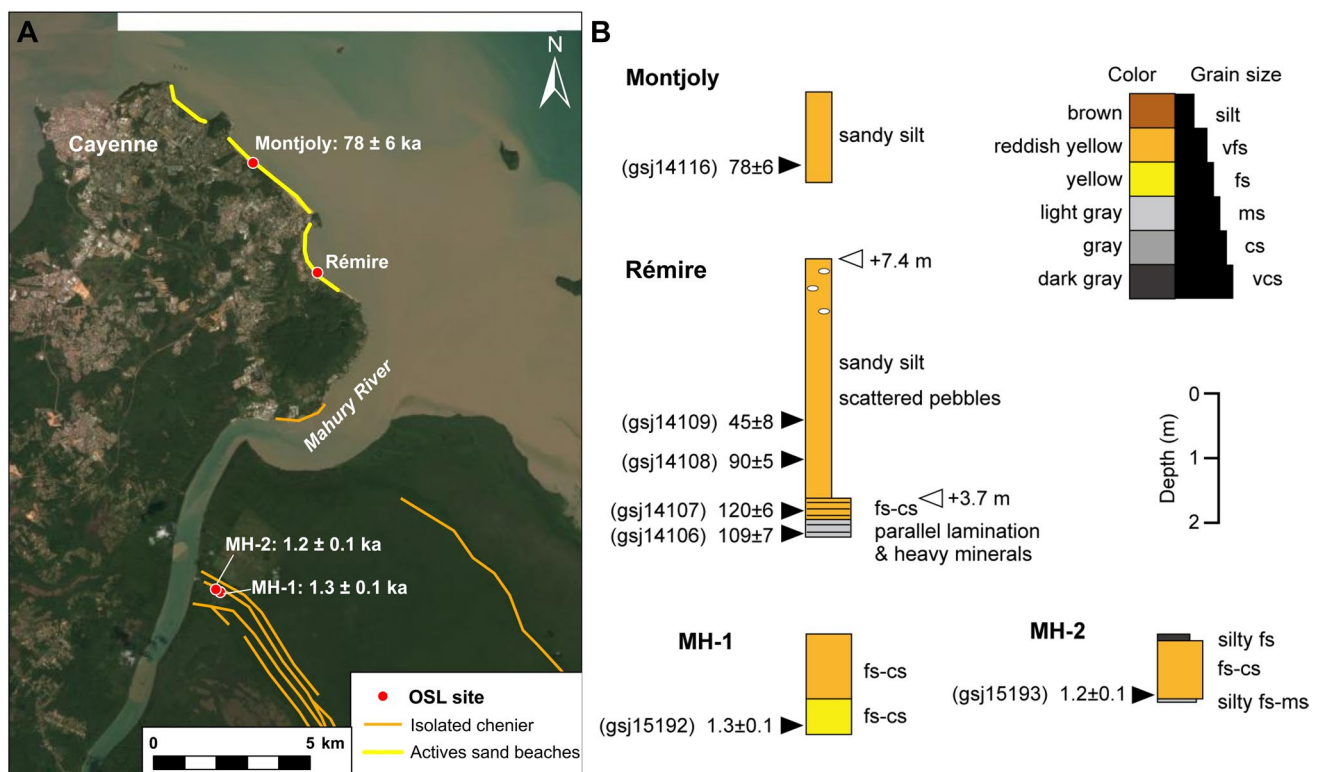

Fig. 4 (**A**) SPOT 6 satellite image from 2015 of the Cayenne area; the bedrock Cayenne Promontory and coastal lowland east of the Mahury River. Locations of optically stimulated luminescence (OSL) sample sites are shown with red points. (**B**) Sediment logs recorded during the auger drilling at MH-1 and MH-2 and characterized by outcrop observation at Montjoly and Remire

drilled at MH-1 and -2 in the landward ridges, revealing stratigraphy characterized by yellow to reddish yellow fine to coarse sand, overlain by a thin dark grey topsoil at MH-2. Samples 15,192 and 15,193 were taken from yellow sand at MH-1 and reddish yellow sand at MH-2, respectively.

The Kourou area is situated between Cayenne and Sinnamary, where the coastal lowland 6–7 km wide, is associated with several chenier ridges. During fieldwork in 2015, the shoreline in Kourou experienced an inter-bank phase characterized by active sandy beach dynamics representing the current chenier in this area (Jolivet et al. 2022). An auger hole was drilled at Kou-1, 100 m inland of the beach (Fig. 1). Reddish yellow fine to medium sand was observed in the Kou-1 hole, from which sample gsj15181 was collected.

Optically stimulated luminescence ages

Bright OSL signals dominated by the fast component were observed for all samples (Fig. S2). D_es of the samples were then determined from well-defined dose–response curves. The De distributions of some samples show very high overdispersion values (Table 1) with a few aliquots of relatively higher D_e values likely reflecting inclusion of poorly-bleached grains. Removing such outlier aliquots is considered to minimize effects of such grains as in other sandy beach settings (e.g. Tamura et al. 2019; Oliver et al. 2020). The only exception is sample gsj14109, collected from the upper part of the massive silt of the Remire section. In this sample, the broad and likely polymodal distribution remains even after excluding an outlier outside the 25th and 75th percentiles, which suggests other mechanism for the variable D_e

Table 1 Optically stimulated luminescence (OSL) dating results: environmental dose rate, equivalent dose (D_e), overdispersion value (OD) after the Central Age Model, numbers of aliquots measured (n) and used for the determination of D_e (n'). OSL ages exceeding 100, 1000, and 10,000 years are rounded to the nearest decade, century, and millennium, respectively

Lab code	Site	Dose rate (Gy/ka)	Equivalent dose (Gy)	OD (%)	n	n'	Age (ka)
La Mahouri & Cayenne							
gsj15192	MH-1	0.47 ± 0.02	0.61 ± 0.03	25	24	15	1.30 ± 0.07
gsj15193	MH-2	0.76 ± 0.03	0.95 ± 0.03	15	24	17	1.25 ± 0.06
gsj14116	Montjoly	1.06 ± 0.04	82.37 ± 5.50	34	16	15	77.74 ± 6.12
gsj14106	Remire	0.74 ± 0.03	80.52 ± 3.54	35	24	20	109.18 ± 6.94
gsj14107	Remire	0.28 ± 0.01	33.15 ± 0.90	15	24	20	120.09 ± 6.09
gsj14108	Remire	1.29 ± 0.06	116.01 ± 4.28	21	16	14	90.16 ± 5.20
gsj14109	Remire	1.15 ± 0.05	51.89 ± 8.57	64	16	14	44.98 ± 7.68
Kourou							
gsj15181	Kou-1	0.49 ± 0.02	0.18 ± 0.01	38	24	17	0.37 ± 0.02
Sinnamary							
gsj14103	Sinnamary-1	1.36 ± 0.06	170.70 ± 6.50	14	16	16	125.27 ± 7.37
gsj14104	Sinnamary-2	0.46 ± 0.02	3.18 ± 0.22	54	34	18	6.96 ± 0.54
gsj14105	Sinnamary-3	1.35 ± 0.06	139.61 ± 5.07	17	16	14	103.14 ± 5.87
gsj15182	Sinnamary-4	0.69 ± 0.03	0.18 ± 0.02	63	24	20	0.27 ± 0.03
Irracoubo							
gsj15170	Ira-1	18.96 ± 1.08	11.56 ± 0.54	32	24	17	0.61 ± 0.05
gsj15172	Ira-3	5.68 ± 0.30	8.74 ± 0.26	18	24	19	1.54 ± 0.09
gsj15173	Ira-4	0.74 ± 0.03	0.57 ± 0.02	42	24	11	0.76 ± 0.04
gsj15174	Ira-4	0.57 ± 0.02	0.55 ± 0.02	26	24	19	0.96 ± 0.05
Yalimapoo to Mana Polder							
gsj15179	Mana-21	0.84 ± 0.03	0.37 ± 0.02	33	24	23	0.44 ± 0.03
gsj15180	Mana-22	0.33 ± 0.01	0.35 ± 0.01	12	24	20	1.07 ± 0.04
gsj14113	Awala-1	0.95 ± 0.04	1.36 ± 0.06	20	24	20	1.43 ± 0.09
gsj15190	Awala-3	1.03 ± 0.05	0.99 ± 0.04	54	24	18	0.96 ± 0.06
gsj15191	Awala-4	0.70 ± 0.03	1.00 ± 0.03	16	24	22	1.44 ± 0.07
gsj14110	Yali-1	0.35 ± 0.01	1.83 ± 0.05	14	24	22	5.32 ± 0.25
gsj14111	Yali-2	1.09 ± 0.05	4.43 ± 0.07	18	24	20	4.05 ± 0.20
gsj14112	Yali-3	0.45 ± 0.02	1.84 ± 0.03	14	24	18	4.05 ± 0.16
gsj15187	Yali-21	0.48 ± 0.02	2.04 ± 0.03	10	24	14	4.28 ± 0.18
gsj15188	Yali-22	0.68 ± 0.03	1.94 ± 0.04	13	24	22	2.83 ± 0.13
gsj15189	Yali-23	1.92 ± 0.10	1.04 ± 0.02	15	24	20	0.55 ± 0.03
gsj14115	Sim-1	0.33 ± 0.01	0.66 ± 0.02	22	24	19	2.01 ± 0.10

of grains, such as post-depositional mixing. The final OSL age of this sample may, thus, be less reliable. The dose rate of individual samples is highly variable; even if samples gsj15170 and 15,172 with extremely high contents of U and Th are excluded, it shows a wide range 0.28–1.92 Gy/ka (Tables 1, S1). This does not reflect inter-area variations but occurs even within a single area, largely owing to variable contents of radionuclides. The variable contents may be partly accounted for by elemental migration in the sediment after deposition as also indicated by the podzol development in chenier sands (Fig. 4B). This suggests that the apparent dose rate determined in the laboratory is not strictly equivalent to the average rate over the duration of deposition.

Of the 28 samples, 21 were dated younger than 7 ka (Table 1; Figs. 1–4). These ages are largely consistent with the morphostratigraphy revealed by chenier ridges in each area. The remaining seven samples were derived from exposures in the Cayenne Promontory and Sinnamary and dated as Late Pleistocene.

Five OSL ages were in the range of 2.8–5.3 ka in a series of chenier ridges near the mouth of the Maroni River in the Awala area (Fig. 2). The age of sample gsj15188, 2.8 ± 0.1 ka, is exceptionally young and is considered to reflect human-induced sediment reworking as suggested by the unusually thick organic topsoil and associated pottery fragments. Thus, this sample is not considered further. Three of the remaining four ages are consistent, in the range of 4.1–4.3 ka, but sample gsj14110 at Yali-1, the most seaward site that should be considered youngest, was dated oldest (5.3 ± 0.3 ka). Although these four ages represent a slight age reversal, the chenier ridges along the Maroni River are considered to have been formed around the middle Holocene (4.5 ± 0.6 ka on average). Sample gsj15189 from the levee of the abandoned Mana river channel was dated 0.55 ± 0.03 ka, suggesting that this channel course was active until recently. OSL ages ranging from 1.0 to 2.0 ka were determined from the seaward shore-parallel ridges, except for sample gsj15179, dated 0.44 ± 0.03 ka, exceptionally younger than other samples. This young age is derived from a similar D_e with sample 15,180 at Mana-22 nearby and a relatively high dose rate due to high concentrations of U and Th (Tables 1, S1) that might have been potentially affected by post-depositional dose-rate alteration. Three OSL ages at Awala-1, -3, and -4 reveal a slight inconsistency with the morpho-stratigraphy; sample gsj15190 (1.0 ± 0.1 ka) at Awala-3, in the middle, is slightly younger than sample14113 (1.4 ± 0.1 ka) at Awala-1 on the seaward part of the ridge. Considering the likely effect of the post-depositional dose rate change, rather than the detailed chronology, we may estimate the approximate timing of the ridge formation from the average of six OSL ages obtained from the shore-parallel ridges at 1.2 ± 0.5 ka. These two clusters of chenier ridges in the Awala area thus formed discontinuously, illustrating the sporadic nature of muddy coastal advance and chenier formation after the middle Holocene.

OSL ages determined in the Irracoubo and Sinnamary areas are generally young except for three ages at the west bank of the Sinnamary River (Fig. 3). Both of Ira-1 and Ira-3 are located in the ridge defining the landward margin of the coastal plain, and their samples (gsj15170 and 15,172) were dated as young as 0.61 ± 0.05 and 1.5 ± 0.1 ka. Two ages at Ira-4 (gsj15173 and 15,174) in the ridge seaward of Ira-3 were 0.76 ± 0.04 and 1.0 ± 0.1 ka, respectively. The average of these four ages is 1.0 ± 0.1 ka, approximately corresponding to the timing of the shore-parallel ridge in the Awala area. A very young OSL age was determined for sample gsj15182 at Sinnamary-4 in the ridge defining the landward end of the coastal plain at the east bank of the Sinnamary River. Other three ages were determined for the shore-parallel chenier ridges at the west bank of the Sinnamary River. Samples gsj14103 and 14,105, collected from the basal silty layer in boreholes at Sinnmary-1 and -3, were dated 125 ± 7 and 103 ± 6 ka, the Last Interglacial period. Sample 14,104 from reddish sand at Sinnamry-2, of which the auger hole did not reach the basal silt, was dated 7.0 ± 0.5 ka. These chronostratigraphic features support an interpretation that the silt layer of the Last Interglacial period is the basement that was transgressed during the post-glacial sea-level rise and subsequently overlain by the chenier sand composed of reddish-yellow sand comprising leached sand during the initial advance of the coast.

The outcrop sections in the Cayenne Promontory are characterized by five Late Pleistocene OSL ages (Fig. 4). Two samples (gsj14106 and 14,107) from the beach deposits in the Remire section were dated 109 ± 7 and 120 ± 7 ka. The beach deposits are, thus, considered indicating the sea level highstand of the Last Interglacial. Two ages (gsj14108 and 14,109) from the sandy silt overlying the beach deposits were 90 ± 5 and 45 ± 8 ka, correlated with the OSL age (gsj14116) from sandy silt in Monjoly beach (78 ± 6 ka). The sandy silt does not show evidence of fluvial or marine deposition and thus is interpreted as loess that accumulated over the beach deposits when the sea level fell following the Last Interglacial highstand. Two chenier sand samples (gsj15192 and 15,193) collected at MH-1 and MH-2, c. 10 km inland from the present shoreline, were dated 1.3 ± 0.1 and 1.2 ± 0.1 ka, respectively. Their average is 1.3 ± 0.1 ka, also corresponding to the shore-normal ridges in the Awala and Iracoubo areas. One sample (gsj15181) from the chenier ridge close to the shoreline in Kourou was dated 0.37 ± 0.02 ka, close to the age at Sinnamary 4.

Discussion

The OSL ages of the French Guiana coastal plain and their spatial distribution provide a framework for interpreting the long-term evolution of the coast and the dynamics of shoreline mobility in response to the alongshore passage of mud banks separated by inter-bank areas. The ages show, notably, the preservation of Late Pleistocene deposits in

a context that may have been similar to that of the Late Holocene. They also indicate distinct phases of reworking of locally derived sandy fluvial deposits in a regional larger-scale sedimentary system dominated by mud massively supplied by the distant mouths of the Amazon and transported alongshore. These themes are discussed below.

Pleistocene deposits

Seven ages record the preservation, in places, of residual coastal and terrigenous deposits of Late Pleistocene age (45–120 ka). In the Cayenne area, the bedrock promontory preserves the Last Interglacial high sea-level stand beaches that are now fronted by the Holocene to modern beach deposits (Figs. 2C, 4). These beaches form relatively narrow bodies in Montjoly, Remire, and smaller pocket beaches encased between bedrock headlands. This stratigraphic relationship suggests that beaches during both Pleistocene and Holocene sea-level highstands were formed in a similar sand-deficient context, probably reflecting the same conditions of Amazon mud-dominated coastal sedimentation that prevailed during the Holocene. Anthony and Dolique (2004) attributed this limited development of beach deposits to both the small size of river catchments in the Cayenne area and the blanketing of sand deposited by these rivers on the inner continental shelf during sea-level fall by active deposition of mud offshore and supply of mud from the Amazon during highstand phases, including the present. The Mahury has a small catchment (area: 1760 km^2), which has been a limiting factor in terms of fluvial sand supply. In this context, the Pleistocene highstand beaches in Remire and perhaps Montjoly, backed by bedrock outcrops and older Pleistocene deposits formed during the Last Interglacial (Brinkman and Pons, 1968), were preserved during the Late Pleistocene sea-level fall during which they were capped by some aeolian deposition, as suggested by the three ages from overlying sandy silt ranging in age from 45 to 90 ka. In the Sinnamary area where bedrock does not crop out, the late Pleistocene shoreline was probably truncated and segmented. The preservation of these Late Pleistocene shorelines in both the Cayenne and Sinnamary areas clearly indicates that they have not been completely reworked by waves at the height of the Holocene sea-level highstand.

Holocene cheniers and river dynamics

The lithology of the chenier sands in French Guiana indicates that they are fluvially sourced, notably by the Mana and other smaller rivers in French Guiana that drain the Guiana Shield (Anthony et al. 2013). In addition to sand

sourcing by the coastal rivers, reworking of old abandoned cheniers inland during prolonged inter-bank phases may also have led to sand releases to the shore. The OSL ages show the preponderance of Holocene cheniers that exhibit in places a complex spatial distribution of the ages.

The Holocene cheniers in central and western French Guiana have developed in an open-beach context. Still, they have been subject to significant reworking by waves during inter-bank phases and by changes in river courses and river-mouth locations that also reflect the overarching influence of mud-bank and inter-bank dynamics. Mud banks are the essential control on the seaward growth of the coastal plain, with cheniers simply representing the imprint of the reworking of fluvial sandy deposits, or older cheniers, during inter-bank (relatively mud-deficient) phases. The combination of Amazon modulation of mud supply with inter-bank muddy erosion along the French Guiana coast has been shown to result in changes in the courses of the smaller Iracoubo, Sinnamary, and Mana Rivers west of the large stable mouth of the much bigger Maroni River catchment (Jolivet et al. 2019a, 2019b; Gardel et al. 2021). Jolivet et al. (2019a) documented, for instance, over the period 1955–2017, the demise of Pointe Isère in western French Guiana (Fig. 2A), involving a loss of 41.8 km^2 of coastal plain composed essentially of mangrove wetlands, which resulted in the eastward relocation of the mouth of the Mana River. The large mud cape of Pointe Isère had diverted the Mana River westwards up to 2011 since at least the nineteenth century (Plaziat and Augustinus 2004), and remnants of this cape form a shore-attached mangrove-bearing feature. The gradual impingement of a large mud bank was accompanied, in 2011, by sealing of the ancestral mouth of the Mana by mud and deflection of the present mouth of this river several kilometres east of the village of Awala, which is now completely isolated from the sea by the shore-attached remnant of Pointe Isère. Such changes result in significant variability in the alongshore formation or reworking of cheniers (Brunier et al. 2019) and provide a template for considering the range of OSL ages associated with chenier outcrops. Two good examples of river reworking are found in the Awala area. The shore-parallel ridges (c. 1.2 ± 0.5 ka, the average of five OSL ages) are partly truncated by a meander of the Mana River, and a series of ridges along the Maroni River (4.5 ± 0.6 ka, the average of four OSL ages) show abrupt truncations at their eastern ends that appear to have been caused by a now abandoned river channel course. These examples reveal how the reworking of cheniers can be caused by the deflections of the small French Guiana rivers associated with the migration of mud banks even thousands of years after chenier formation.

Holocene chenier clusters and phases of formation

OSL ages of Holocene cheniers determined in this area, although containing a few reversals, appear to define three clusters (Fig. S5). The first cluster is identified along the

Maroni River and centred on 4.5 ± 0.6 ka. The second cluster, the average age of which is 1.0–1.3 ka, is prominent and common to three areas, Awala, Irracoubo, and Mahury, east of Cayenne, thus illustrating a good degree of inter-bank chenier formation in French Guiana within the same age range. The third cluster is defined by the recent cheniers in the Kourou and Sinnamary areas, averaged at 0.32 ± 0.07 ka. The prominent cluster at 1.0–1.3 ka reveals a clear hiatus with the older cluster in the Awala area, defines the landward margin of the Holocene chenier plain in the Irracoubo area, and occurs in the landward part of the Holocene plain along the east bank of the Mahury River. The age of this cluster indicates that in spite of the prolonged sea-level stillstand over the last 6–7 thousand years (Milne et al. 2005), much of the present muddy coastal plain may have been formed and preserved after 1.0–1.3 ka in French Guiana. This may imply that either coastal advance prior to 1.0–1.3 ka was negligible or a pre-existing muddy coastal plain was largely eroded during the course of the phase of formation of the cluster at 1.0–1.3 ka, except east of the Mahury River where the existing plain is up to 25 km wide. Given the dynamic nature of the French Guiana coast and the possibility of large-scale changes and, consequently, massive periodic erosion such as recently documented by Jolivet et al. (2019a), as mentioned above, the possibility of massive removal of much of the muddy coastal plain is more likely. Large-scale preservation of muddy deposits appears to have been the prevailing condition in the eastern confines of French Guiana (Fig. 4) and Amapa in Brazil. In this area, massive muddy sedimentation has formed mud capes associated with river mouths (Gardel et al. 2022). These mud capes comprise undated cheniers. The position of cheniers defining the prominent cluster in French Guiana is thus considered to suggest the millennial-scale instability of this coast. The phases of massive muddy coastal advance or erosion in French Guiana are embedded in the large-scale regional sediment dynamics of the Amazon-influenced Guianas coast, wherein mud deposited and subsequently eroded is transported westwards towards the mouths of the Orinoco, the terminus of the mud-bank system, contributing to the growth of the Orinoco deltaic complex and its deep-sea fan (Peng et al. 2018).

Information for constraining causes of the shoreline retreat at 1.0–1.3 ka is limited. The retreat could be related to a single prolonged inter-bank phase and/or an episode dominated by inter-bank phases over bank phases. However, little is known of long-term fluctuations in sedimentation controlled by the sediment sequestration and release processes operating at the mouths of the Amazon, the largest river-mouth to marine-transition zone on Earth (Nittrouer et al. 2021), but arguably also the most complex one. Sedimentation at the mouths of the Amazon is, in the first place, hinged on sediment supply at the scale of the large river catchment. Wittmann et al. (2011) showed from cosmogenic

nuclide-derived sedimentation rates at Obidos, a discharge-gauging station 800 km upstream of the mouths of the Amazon, that sediment loads from the basin to the sea have been relatively constant, despite potential fluctuations related to climatic variations and anthropogenic perturbations, which are buffered by the large Amazon floodplain. While the Holocene catchment sediment supply issue still needs to be more thoroughly understood, it is likely, given the large mud load exiting at the mouths of the Amazon, that the proportion migrating along the Guianas coast, estimated at about 30% (Eisma et al. 1991), will be modulated by subaqueous sediment-routing processes off the mouths of the river and by the ocean–atmosphere interactions that lead to alongshore mobility northwestwards, a latter component that is poorly known. Sommerfield et al. (1995) suggested along-shelf variations in sediment dispersal hinged on the importance of deposition versus erosion at the mouths of the Amazon that should directly impact the Guianas coast. Interestingly, based on limited chronology derived from radiocarbon dating and Pb-210 activity, Sommerfield et al. (1995) identified a sediment accumulation phase between > 1800 and 700 yr BP on the shelf and an erosional phase between 700 yr BP and 100 yr ago, followed by an accumulation phase until the present. These authors further suggested that during the erosional phase at the Amapa coast just north of the mouths of the Amazon, the downdrift Guianas coast served as a depocentre. Paleoenvironmental studies in the Amazon-influenced region with a refined chronology are still needed to throw further light on these sediment-partitioning problems. Along the rest of the Amazon-influenced coast, millennial-scale variability in mud preservation could have been generated by regional coastal orientation, river-mouth hydrology, and adjacent sediment accommodation space.

The remaining two clusters of chenier OSL ages also provide useful information on the coastal dynamics. The older cluster identified along the east bank of the Maroni River survived the erosion at 1.0–1.3 ka. These cheniers formed during the initial phase of coastal advance in response to the Holocene sea-level stillstand. Their E-W orientation, in contrast to other cheniers stretching NW–SE, can be attributed to more ample sediment accommodation space in the vicinity of the river mouth that offered protection of the cheniers from erosion or to recurves along the banks of the Maroni associated with wave refraction as envisaged by Gardel et al. (2021). The cheniers at the left bank of the Sinnamary River, where an older Holocene age (7.0 ± 0.5 ka) was determined for Sinnamary-2, also survived the erosion at 1.0–1.3 ka, but are not associated with ample accommodation space. The preservation of these cheniers may, thus, be related to conditions specific to the westward deflection of the Sinnamary River by muddy coastal-plain advance. The younger cluster defined by cheniers in Kourou and Sinnamary may represent the relatively large-scale retreat in a centennial time scale

although this was not as pronounced as the one at 1.0–1.3 ka. The distribution and OSL ages of cheniers in French Guiana provide valuable insights into the multi-timescale stability and instability of this dynamic coastline. The recent multi-decadal changes associated with the Mana River outlet and the shoreline show, for instance, that (1) the complexity of shoreline reworking can lead to the juxtaposition of chenier segments of widely differing age along a same segment of shoreline and (2) timescales of muddy shoreline advance or inter-bank erosion can be long and unpredictable, determined by processes of mud release from the distant mouths of the Amazon and by alongshore variability in conditions favourable or not to large-scale mud storage.

Conclusions

Twenty-eight optically stimulated luminescence ages obtained on the cheniers and associated coastal deposits in French Guiana provide valuable insight into the multi-timescale stability and instability of this dynamic coastline. The ages are largely consistent with the morpho-stratigraphy of the chenier ridges in three areas of the French Guiana coast, defining three clusters of Holocene chenier formation centred on 4.5 ± 0.6 ka, 1.0–1.3 ka, and 0.32 ± 0.07 ka, and, additionally, localized Pleistocene shoreline deposits related to the Last Interglacial sea-level highstand. The Holocene ages indicate synchroneity of chenier formation phases that have been significantly influenced by alongshore diversions of river mouths and changes in river-mouth position over time associated with the overarching net muddy sedimentation on the coastal plain. A regional time frame of chenier formation can be corroborated by a larger collection of dates covering notably the neighbouring coasts of Suriname where abundant cheniers line the coast, and that of Amapa, in Brazil, where cheniers are sparser but associated with large mud capes diverting river mouths. By informing on patterns of coastal advance and erosion, the results obtained from OSL ages in French Guiana could have broader implications for shoreline management and coastal land-use planning throughout the muddy Guianas coast between the mouths of the Amazon and Orinoco rivers.

Declarations

References

Adamiec G, Aitken M (1998) Dose-rate conversion factors: update. Ancient TL 16:37–50

Allison MA, Lee MT (2004) Sediment exchange between amazon mudbanks and fringing mangroves in French Guiana. Mar Geol 208:169–190. https://doi.org/10.1016/j.margeo.2004.04.026

Anthony EJ (1989) Chenier plain development in northern Sierra Leone, West Africa. Mar Geol 90:297–309. https://doi.org/10.1016/0025-3227(89)90132-1

Anthony EJ, Dolique F (2004) The influence of Amazon-derived mud banks on the morphology of sandy, headland-bound beaches in Cayenne, French Guiana: a short- to long-term perspective. Mar Geol 208:249–264. https://doi.org/10.1016/j.margeo.2004.04.011

Anthony EJ, Gardel A, Gratiot N, Proisy C, Allison MA et al (2010) The Amazon-influenced muddy coast of South America: a review of mud-bank-shoreline interactions. Earth-Science Rev 103:99–121. https://doi.org/10.1016/j.earscirev.2010.09.008

Anthony EJ, Gardel A, Proisy C, Fromard F, Gensac E et al (2013) The role of fluvial sediment supply and river-mouth hydrology in the dynamics of the muddy, Amazon-dominated Amapá-Guianas coast, South America: a three-point research agenda. J S Am Earth Sci 44:18–24. https://doi.org/10.1016/j.jsames.2012.06.005

Anthony EJ, Gardel A, Gratiot N (2014) Fluvial sediment supply, mud banks, cheniers and the morphodynamics of the coast of South America between the Amazon and Orinoco river mouths. Geol. Soc., Lon. Special Publications 388:533–560. https://doi.org/10.1144/sp388.8

Anthony EJ, Brunier G, Gardel A, Hiwat M (2019) Chenier morphodynamics and degradation on the Amazon-influenced coast of Suriname, South America: implications for beach ecosystem services. Front Earth Sci 7:35. https://doi.org/10.3389/feart.2019.00035

Augustinus PGEF (1978) The changing shoreline of Suriname (South America). Diss. University Utrecht

Augustinus PG (2004) The influence of the trade winds on the coastal development of the Guianas at various scale levels: a synthesis. Mar Geol 208:141–151. https://doi.org/10.1016/j.margeo.2004.04.007

Augustinus PG, Hazelhoff L, Kroon A (1989) The chenier coast of Suriname: modern and geological development. Mar Geol 90:269–281. https://doi.org/10.1016/0025-3227(89)90129-1

Banerjee D, Murray AS, Bøtter-Jensen L, Lang A (2001) Equivalent dose estimation using a single aliquot of polymineral fine grains. Radiat Meas 33:73–94. https://doi.org/10.1016/S1350-4487(00)00101-3

Bateman MD, Catt JA (1996) An absolute chronology for the raised beach deposits at Sewerby, E. Yorkshire. UK J Quat Sci 11:389–395. https://doi.org/10.1002/(SICI)1099-1417(199609/10)11:5%3c389::AID-JQS260%3e3.0.CO;2-K

Boulter C, Bateman MD, Frederick CD (2010) Understanding geomorphic responses to environmental change: a 19 000-year case study from semi-arid central Texas, USA. J Quaternary Sci 25:889–902. https://doi.org/10.1002/jqs.1365

Brinkman R, Pons LJ (1968) A pedo-geomorphological classification and map of the Holocene sediments in the coastal plain of the three Guianas. Soil Survey Papers 4, 41 pp.

Brunier G, Anthony EJ, Gratiot N, Gardel A (2019) Exceptional rates and mechanisms of muddy shoreline retreat following mangrove removal. Earth Surf Proc Land 44:1559–1571. https://doi.org/10.1002/esp.4593

Daniel JRK (1989) The chenier plain coastal system of Guyana. Mar Geol 90:283–287. https://doi.org/10.1016/0025-3227(89)90130-8

Eisma D, Augustinus PGEF, Alexander CR (1991) Recent and subrecent changes in the dispersal of Amazon mud. Netherlands J Sea Res 28:181–192. https://doi.org/10.1016/0077-7579(91)90016-T

Galbraith RF, Roberts RG, Laslett GM, Yoshida H, Olley JM (1999) Optical dating of single and multiple grains of quartz from Jinmium rock shelter, northern Australia: Part I, experimental design and statistical models. Archaeometry 41:339–364. https://doi.org/10.1111/j.1475-4754.1999.tb00987.x

Gardel A, Gratiot N (2005) A satellite image-based method for estimating rates of mud bank migration, French Guiana, South America. J Coast Res 21:720–728. https://doi.org/10.2112/03-0100.1

Gardel A, Anthony EJ, Ferreira dos Santos V, Huybrechts N, Lesourd S et al (2021) Fluvial sand, Amazon mud, and sediment accommodation in the tropical Maroni River estuary: controls on the transition from estuary to delta and chenier plain. Reg Stud Mar Sci 41:101–548. https://doi.org/10.1016/j.rsma.2020.101548

Gardel A, Anthony EJ, dos Santos VF, Huybrechts N, Lesourd S, Sottolichio A, Maury T (2022) A remote sensing-based classification approach for river mouths of the Amazon-influenced Guianas coast. Reg Environ Chang 22:3. https://doi.org/10.1007/s10113-022-01913-3

Gratiot N, Gardel A, Anthony EJ (2007) Trade-wind waves and mud dynamics on the French Guiana coast, South America: input from ERA-40 wave data and field investigations. Mar Geol 236:15–26. https://doi.org/10.1016/j.margeo.2006.09.013

Hein CJ, Fitzgerald DM, de Souza LHP, Georgious JY, Buynevich IV et al (2016) Complex coastal change in response to autogenic basin infilling: an example from a sub-tropical Holocene strandplain. Sedimentology 63:1362–1395. https://doi.org/10.1111/sed.12265

Hori K, Saito Y, Zhao Q, Cheng X, Wang P et al (2001) Sedimentary facies and Holocene progradation rates of the Changjiang (Yangtze) delta, China. Geomorph 41:233–248. https://doi.org/10.1016/S0169-555X(01)00119-2

Janjou D (2004) Descriptif des cartes géologiques à 1/50 000 format "vecteurs". BRGM/RP-53473-FR, 21 p.

Jolivet M, Anthony EJ, Gardel A, Brunier G (2019) Multi-decadal to short-term beach and shoreline mobility in a complex river-mouth environment affected by mud from the Amazon. Front Earth Sci 7:1–17. https://doi.org/10.3389/feart.2019.00187

Jolivet M, Gardel A, Anthony EJ (2019) Multi-decadal changes on the mud-dominated coast of western French Guiana: implications for mesoscale shoreline mobility, river-mouth deflection, and sediment sorting. J Coast Res Special Issue 88:185–194. https://doi.org/10.2112/SI88-014.1

Jolivet M, Anthony EJ, Gardel A, Maury T, Morvan S (2022) Dynamics of mud banks and sandy urban beaches in French Guiana, South America. Reg Environ Chang 22. https://doi.org/10.1007/s10113-022-01944-w

McBride RA, Taylor MJ, Byrnes MR (2007) Coastal morphodynamics and chenier-plain evolution in southwestern Louisiana, USA: a geomorphic model. Geomorph 88:367–342. https://doi.org/10.1016/j.geomorph.2006.11.013

Milne GA, Long AJ, Bassett SE (2005) Modelling Holocene relative sea-level observations from the Caribbean and South America. Quaternary Sci Rev 24:1183–1202. https://doi.org/10.1016/j.quascirev.2004.10.005

Murray AS, Wintle AG (2000) Luminescence dating of quartz using an improved single-aliquot regenerative-dose protocol. Radiat Meas 32:57–73. https://doi.org/10.1016/S1350-4487(99)00253-X

Nardin W, Fagherazzi S (2018) The role of waves, shelf slope, and sediment characteristics on the development of erosional chenier plains. Geophys Res Letters 45. https://doi.org/10.1029/2018GL078694

Nittrouer CA, DeMaster DJ, Kuehl SA, Figueiredo AG Jr, Sternberg RW et al (2021) Amazon sediment transport and accumulation along the continuum of mixed fluvial and marine processes. Annu Rev Mar Sci 13:61–636. https://doi.org/10.1146/annurev-marine-010816-060457

Oliver TS, Tamura T, Brooke BP, Short AD, Kinsela MA, et al. (2020) Holocene evolution of the wave-dominated embayed Moruya coastline, southeastern Australia: sediment sources, transport rates and alongshore interconnectivity. Quat Sci Rev 247:106566. https://doi.org/10.1016/j.quascirev.2020.106566

Otvos EG (2018) Cheniers. In: Finkl C & Makowski C (eds.), Encyclopaedia of Coastal Science, Springer. https://doi.org/10.1007/978-3-319-48657-4_67-5

Otvos EG, Price WA (1979) Problems of chenier genesis and terminology: an overview. Mar Geol 31:251–263. https://doi.org/10.1016/0025-3227(79)90036-7

Peng Y, Steel RJ, Cornel O (2018) Amazon fluid mud impact on tide- and wave-dominated Pliocene lobes of the Orinoco Delta. Mar Geol 406:57–71. https://doi.org/10.1016/j.margeo.2018.08.009

Plaziat JC, Augustinus PG (2004) Evolution of progradation/erosion along the French Guiana mangrove coast: a comparison of mapped shorelines since the 18th century with Holocene data. Mar Geol 208:127–143. https://doi.org/10.1016/j.margeo.2004.04.006

Prescott JR, Hutton JT (1994) Cosmic ray contributions to dose rates for luminescence and ESR dating: large depths and long-term time variations. Radiat Meas 23:497–500. https://doi.org/10.1016/1350-4487(94)90086-8

Prost MT (1989) Coastal dynamics and chenier sands in French Guiana. Mar Geol 90:259–267. https://doi.org/10.1016/0025-3227(89)90128-X

Roeleveld W, Van Loon AJ (1979) The Holocene development of the young coastal plain of Suriname. Geol En Mijnbouw 58:21–28

Saito Y, Wei H, Zhou Y, Nishimura A, Sato Y et al (2000) Delta progradation and chenier formation in the Huanghe (Yellow River) delta, China. J Asian Earth Sci 18:489–497. https://doi.org/10.1016/S1367-9120(99)00080-210.1016/S1367-9120(99)00080-2

Scheffers A, Engel M, Scheffers S, Squire P, Kelletat D (2012) Beach ridge systems - archives for Holocene coastal events? Prog Phys Geography 36:5–37. https://doi.org/10.1177/0309133311419549

Sommerfield CK, Nittrouer CA, Figueiredo AG (1995) Stratigraphic evidence of changes in Amazon shelf sedimentation during the late Holocene. Mar Geol 125:351–371. https://doi.org/10.1016/0025-3227(95)00019-U

Tamura T (2012) Beach ridges and prograded beach deposits as palaeoenvironment records. Earth-Science Rev 114:279–297. https://doi.org/10.1016/j.earscirev.2012.06.004

Tamura T, Oliver TSN, Cunningham AC, Woodroffe CD (2019) Recurrence of extreme coastal erosion in SE Australia beyond historical timescales inferred from beach ridge morphostratigraphy. Geophys Res Let 46:4705–4714. https://doi.org/10.1029/2019GL083061

Tas S, van Maren DS, Reniers AJHM (2020) Observations of cross-shore chenier dynamics in Demak. Indonesia J Mar Sci & Eng 8:972. https://doi.org/10.3390/jmse8120972

Tas S, van Maren DS, Helmi M, Reniers AJHM (2022) Drivers of cross-shore chenier dynamics off a drowning coastal plain. Mar Geol 445:106753. https://doi.org/10.1016/j.margeo.2022.106753

van Maren DS (2005) Barrier formation on an actively prograding delta system: the Red River Delta. Vietnam Mar Geol 224:123–143. https://doi.org/10.1016/j.margeo.2005.07.008

de Vries J, van Maanen B, Ruessink G, Verweij PA, de Jong SM (2022) Multi-decadal coastline dynamics in Suriname controlled by migrating subtidal mudbanks. Earth Surf Proc Land 1-18. https://doi.org/10.1002/esp.5390

Walcker R, Anthony EJ, Cassou C, Aller RC, Gardel A et al (2015) Fluctuations in the extent of mangroves driven by multi-decadal changes in North Atlantic waves. J Biogeogr 42:2209–2219. https://doi.org/10.1111/jbi.12580

Wells JT, Coleman JM (1981) Physical processes and fine-grained sediment dynamics, coast of Surinam, South America. J Sed Petrol 51:1053–1068

Winterwerp JC, de Graaff RF, Groeneweg J, Luijendijk AP (2007) Modelling of wave damping at Guyana mud coast. Coast Eng 54:249–261. https://doi.org/10.1016/j.coastaleng.2006.08.012

Wittmann H, von Blackenberg F, Maurice L, Guyot JL, Filizola N et al (2011) Sediment production and delivery in the Amazon River basin quantified by in-situ-produced cosmogenic nuclides and recent river loads. Geol Soc Am Bull 123:934–950. https://doi.org/10.1130/B30317.1

Wong ThE, De Kramer R, De Boer PL, Langereis C, Sew-A-Tion J (2009) The influence of sea level changes on tropical coastal wetlands: the Pleistocene Coropina formation, Suriname. Sediment Geol 216:127–137. https://doi.org/10.1016/j.sedgeo.2009.02.003

Woodroffe CD, Grime D (1999) Storm impact and evolution of a mangrove-fringed chenier plain, Shoal Bay, Darwin, Australia. Mar Geol 159:303–321. https://doi.org/10.1016/S0025-3227(99)00006-7

Publisher's note Springer Nature remains neutral with regard to jurisdictional claims in published maps and institutional affiliations.